Journal of proteome research

Article

pubs.acs.org/jpr

Site-Specific Glycan-Peptide Analysis for Determination of *N*-Glycoproteome Heterogeneity

Benjamin L. Parker,[*,†,○] Morten Thaysen-Andersen,[‡] Nestor Solis,[§] Nichollas E. Scott,[§,▽] Martin R. Larsen,[∥] Mark E. Graham,[⊥] Nicolle H. Packer,[‡] and Stuart J. Cordwell[†,§]

[†]Discipline of Pathology, School of Medical Sciences, The University of Sydney, Sydney 2006, Australia

[‡]Department of Chemistry and Biomolecular Sciences, Macquarie University, North Ryde 2106, Australia

[§]School of Molecular Bioscience, The University of Sydney, Sydney 2006, Australia

[∥]Department of Biochemistry and Molecular Biology, The University of Southern Denmark, DK-5230, Denmark

[⊥]Cell Signalling Unit, Children's Medical Research Institute, Westmead 2145, Australia

Supporting Information

ABSTRACT: A combined glycomics and glycoproteomics strategy was developed for the site-specific analysis of *N*-linked glycosylation heterogeneity from a complex mammalian protein mixture. Initially, global characterization of the *N*-glycome was performed using porous graphitized carbon liquid chromatography−tandem mass spectrometry (PGC-LC−MS/MS) and the data used to create an *N*-glycan modification database. In the next step, tryptic glycopeptides were enriched using zwitterionic hydrophilic interaction liquid chromatography (Zic-HILIC) and fractionated by reversed-phase liquid chromatography (RPLC; pH 7.9). The resulting fractions were each separated into two equal aliquots. The first set of aliquots were treated with peptide-*N*-glycosidase F (PNGase F) to remove *N*-glycans and the former *N*-glycopeptides analyzed by nano-RPLC-MS/MS (pH 2.7) and identified by Mascot database search. This enabled the creation of a glycopeptide-centric concatenated database for each fraction. The second set of aliquots was analyzed directly by nanoRPLC-MS/MS (pH 2.7), employing fragmentation by CID and HCD. The assignment of glycan compositions to peptide sequences was achieved by searching the *N*-glycopeptide HCD MS/MS spectra against the glycopeptide-centric concatenated databases employing the *N*-glycan modification database. CID spectra were used to assign glycan structures identified in the glycomic analysis to peptide sequences. This multidimensional approach allowed confident identification of 863 unique intact *N*-linked glycopeptides from 161 rat brain glycoproteins.

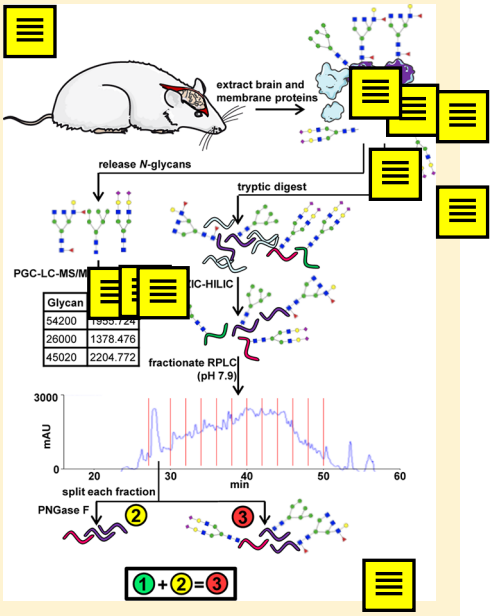

KEYWORDS: *N-linked glycosylation, glycomics, glycoproteomics, mass spectrometry, glycopeptide*

INTRODUCTION

Protein glycosylation has been studied for over 50 years. Despite the first characterization of *N*-linked sugars being performed on ovalbumin by Neuberger and co-workers in 1961,[1] glycosylation profiling has since been performed on only a small fraction of known glycoproteins. The heterogeneous nature of protein glycosylation means that a single polypeptide backbone can be modified with several different oligosaccharide structures (here termed 'glycans') that comprise varying monosaccharide compositions, resulting in different protein 'glycoforms'. A well characterized example of heterogeneity is the *N*-glycosylation of human immunoglobulins, which usually contain core α1,6 fucose (Fuc), none-to-two galactose (Gal) residues, occasionally α2,6 sialic acids (Sia), and a minor amounts of bisecting *N*-acetylglucosamine (GlcNAc).[2,3] This heterogeneity contributes to the efficacy and cytotoxicity of therapeutic antibodies[4,5] and regulates protein interactions, cellular location, and, ultimately, function. Furthermore, glycosylation heterogeneity has the potential to influence a variety of cellular processes including cell adhesion and cell−cell communication,[6−8] protein folding, stability, translocation and secretion,[9−11] and differentiation and organ development.[12,13] A prerequisite for a functional description of every glycoprotein in the proteome is knowledge of both the site(s) of glycan attachment and elucidation of the chemical structures of each glycan that can occupy those sites.

Characterization of the glycans attached to a glycosylation site is only feasible by analysis of intact glycopeptides (or glycoproteins), which to date has remained extremely challenging on a glycoproteome scale. The primary reason for this difficulty lies in the enormous complexity of protein−

Received: July 31, 2013
Published: October 3, 2013

   dx.doi.org/10.1021/pr400783j | *J. Proteome Res.* 2013, 12, 5791−5800

glycan combinations. Consequently, the global analysis of protein glycosylation using mass spectrometry (MS) is typically performed by: (i) glycoproteomics, where the glycoproteins and site(s) of attachment are identified from deglycosylated peptides;[14−16] and (ii) glycomics, where released glycans are characterized without reference to their (former) attachment sites.[17−26] These approaches however, do not provide site-specific information. Site-specific profiling of protein glycosylation is usually performed in a low-throughput manner using purified glycoproteins, which can be analyzed directly by MS, with or without a specific or nonspecific protease, glycosidase treatment, and/or various tandem MS (MS/MS) fragmentation techniques.[27−35] Therefore, only a small fraction of known glycoproteins have been glyco-profiled in a site-specific manner.[36] Few investigators have site-specifically identified peptides with attached oligosaccharides from complex mammalian protein mixtures through intact glycopeptide analysis,[37−41] and in these studies, glycan heterogeneity was reduced prior to glycopeptide detection. Recent improvements in the global analysis of intact glycopeptides have enabled unambiguous identification of peptide−glycan compositions; however, complete structural characterization has not been achieved.[42,43] Since the sheer number and diversity of protein−glycan combinations are currently unknown, improved analytical techniques are required to generate true site-specific glycan structure assignment on a systems-wide level.

The presented multidimensional approach utilizes a global *N*-glycome characterization followed by parallel analysis of deglycosylated and glycosylated peptides with orthogonal fractionation, complementary MS/MS, and advanced data processing tools for site-specific glycan structure assignment. A complex membrane-associated protein preparation from rat brain was used to demonstrate the utility of the strategy.

EXPERIMENTAL SECTION

Materials

All materials were obtained from Sigma-Aldrich unless otherwise stated.

Extraction of Rat Brain-Derived Membrane-Associated Proteins

Male Lewis rats (250 g) were euthanized using the guidelines set out by the University of Sydney Animal Ethics Committee (Approval no. K20/6-2009/3/5078). Following decapitation, brains were removed, rinsed briefly in ice-cold saline (0.9% (w/v) NaCl, pH 7.4) and snap-frozen in liquid nitrogen. Brain tissue was homogenized in ice-cold 100 mM Na_2CO_3 containing protease inhibitor cocktail (Roche) by tip-probe sonication (3 × 15 s). The homogenate was rotated at 4 °C for 30 min and centrifuged at 100,000 × *g* for 2 h at 4 °C. The supernatant was discarded and the pellet containing membrane-associated proteins resuspended in 6 M urea, 2 M thiourea, 50 mM NH_4HCO_3, and 1% (w/v) SDS, pH 6.8. Proteins were precipitated with chloroform/methanol/H_2O (4:1:3) and stored at −20 °C.

N-Glycan Release and Reduction

N-Glycans were prepared as described previously.[44] Briefly, proteins were resuspended in 6 M urea, 2 M thiourea, 50 mM NH_4HCO_3, pH 6.8, and 10 μg spotted onto a PVDF membrane (Millipore) and allowed to dry overnight. Membranes were blocked with 1% polyvinylpyrrolidone for 5 min and washed with H_2O. Five units of PNGase F were added and incubated overnight at 37 °C. *N*-Glycans were collected and glycosylamines from the reducing terminus removed with 20 mM ammonium acetate, pH 5.0, for 1 h. *N*-Glycans were dried by vacuum centrifugation and reduced by resuspension in 1 M $NaBH_4$ in 50 mM KOH for 3 h at 50 °C. The reaction was neutralized with glacial acetic acid and desalted using cation exchange microcolumns as described previously.[44] *N*-glycans were dried by vacuum centrifugation and resuspended in methanol. Excess methyl borate was removed by vacuum centrifugation. Finally, *N*-glycans were purified using porous graphitized carbon (PGC) microcolumns (Grace) and dried by vacuum centrifugation.[44]

Peptide Preparation and Glycopeptide Enrichment

Five milligrams of membrane-associated proteins were resuspended in 1 mL of 6 M urea, 2 M thiourea, 50 mM NH_4HCO_3, pH 6.8, and reduced with 10 mM dithiothreitol for 1 h followed by alkylation with 25 mM iodoacetamide for 30 min in the dark. The solution was diluted to a final volume of 6 mL with 50 mM NH_4HCO_3, pH 6.8, and digested with 100 μg of trypsin for 12 h at 30 °C. Similar conditions have previously been shown to reduce nonenzymatic deamidation, which is important to decrease the identification of false-positive *N*-glycosylation sites.[45,46] $MgCl_2$ was added to a final concentration of 1 mM and peptides were dephosphorylated with 4000 U of lambda phosphatase and 150 U of antarctic phosphatase (New England Biolabs) for 2 h at 30 °C. The solution was acidified to 2% (v/v) formic acid and centrifuged at 16,000 × *g* for 15 min at 25 °C. The reaction was desalted with hydrophilic−lipophilic-balanced (HLB) solid phase extraction (SPE; Waters) and peptides eluted with 1 mL of 80% (v/v) acetonitrile and 1% (v/v) trifluoroacetic acid. Peptides were loaded onto an in-house zwitterionic Zic-HILIC SPE cartridge containing 80 mg of Zic-HILIC particles (10 μm, 200 Å; Sequant/Merck) packed onto a C8 disk (Empore). The flow-through was collected and passed back through the column an additional two times. The column was washed with 4 mL of 80% (v/v) acetonitrile and 1% (v/v) trifluoroacetic acid. Enriched glycopeptides were eluted with 1 mL 0.1% (v/v) trifluoroacetic acid followed by 100 μL of 25 mM NH_4HCO_3 and finally 100 μL of 50% (v/v) acetonitrile and dried by vacuum centrifugation.

Reversed-Phase High Performance Liquid Chromatography (RPLC) Fractionation of Enriched *N*-Glycopeptides

Enriched glycopeptides were resuspended in water and fractionated off-line on an in-house packed 30 cm × 320 μm C18AQ column (3 μm, 120 Å; Dr Maisch GmbH) using a 1200 Series HPLC (Agilent Technologies). Peptides were loaded onto the column for 10 min and separated on a gradient of 0−40% Solvent B over 50 min and 40−90% Solvent B over 5 min followed by 90% Solvent B for 10 min at a flow of 6 μL/min (Solvent A = 10 mM NH_4HCO_3, pH 7.9; solvent B = 90% (v/v) acetonitrile). The following fractions were collected: fraction 1 was collected from 0−28 min, hereafter followed by 2 min fractions with a final fraction from 50−70 min (13 fractions in total) and dried by vacuum centrifugation.

Analysis of Released *N*-Glycans by Porous Graphitized Carbon Liquid Chromatography-Tandem Mass Spectrometry (PGC-LC−MS/MS)

Released *N*-glycans were resuspended in water and separated on a 10 cm × 200 μm PGC column (Hypercarb, 5 μm; Thermo Scientific) using a 1100 Series HPLC (Agilent

dx.doi.org/10.1021/pr400783j | J. Proteome Res. 2013, 12, 5791−5800

Technologies). *N*-Glycans were loaded onto the column, which was initially equilibrated in Solvent A (10 mM NH_4HCO_3, pH 7.9), and separated using the following gradient of Solvent B (10 mM NH_4HCO_3 in acetonitrile); from 2−16% Solvent B over 45 min and 16−45% solvent B over 20 min followed by 45% Solvent B for 6 min and re-equilibration with Solvent A at a flow of 2 μL/min. The HPLC was coupled directly to an MSD 3D ion-trap XCT Plus mass spectrometer (Agilent Technologies) via electrospray ionization (ESI) operated in negative mode. An MS scan (250−2200 *m*/*z*, MS AGC = $7e^4$) was performed followed by data-dependent CID MS/MS analyses of the three most intense precursors. Parameters for acquiring CID were as follows: dynamic exclusion = disabled, MS/MS fragmentation amplitude = 1 V, smart fragmentation = enabled, and ramp amplitude = 30−200%.

Analysis of Former *N*-Glycopeptides and Intact *N*-Glycopeptides by nanoRPLC−MS/MS

Fractions were resuspended in 10.5 μL of H_2O and 5 μL of the intact *N*-glycopeptides analyzed directly by nanoRPLC−MS/MS. The remaining 5 μL was diluted with 20 mM ammonium bicarbonate (pH 6.9) and deglycosylated with 50 U PNGase F (New England Biolabs). Former *N*-glycopeptides were analyzed by nanoRPLC-MS/MS.

Intact *N*-glycopeptides were separated by reversed phase chromatography on an in-house packed 30 cm × 75 μm Reprosil-Pur C18AQ column (3 μm, 120 Å; Dr. Maisch GmbH) with an integrated PicoFrit ESI emitter (New Objective) using an UltiMate 3000 series HPLC (Dionex). The HPLC gradient was 0−40% solvent B (solvent A = 0.1% formic acid; solvent B = 90% acetonitrile and 0.1% formic acid) over 150 min at a flow of 250 nL/min. Parameters were optimized to inhibit insource fragmentation and were as follows: capillary temperature = 275 °C, source voltage = 2.0 kV, and S-lens RF level = 68%. MS detection was achieved using an LTQ-Orbitrap Velos (Thermo Scientific). An MS scan (700−2000 *m*/*z*; MS AGC = 1×10^6) was recorded in the Orbitrap set at a resolution of 30,000 at 400 *m*/*z* followed by data-dependent CID (detection in the ion trap) and HCD (detection in the Orbitrap) MS/MS analysis of the seven most intense precursors. Parameters for acquiring CID were as follows: activation time = 10 ms, normalized energy = 35, dynamic exclusion = enabled with repeat count 1, exclusion duration = 30 s, maximum injection time = 300 ms, and MS^n AGC = 2×10^4. Parameters for acquiring HCD were as follows: activation time = 0.1 ms, normalized energy = 50, dynamic exclusion = enabled with repeat count 1, resolution = 7500, exclusion duration = 30 s, maximum injection time =500 ms, and MS^n AGC = 2×10^5. Analysis of glycopeptides by CID, HCD, and electron transfer dissociation (ETD) was performed as described above except only the three most intense precursors were selected for fragmentation, and ETD was acquired in the Orbitrap. Parameters for acquiring ETD were as follows: activation time = 85 ms, dynamic exclusion = enabled with repeat count 1, resolution = 7500, exclusion duration = 30 s, maximum injection time = 500 ms, MS^n AGC = 2×10^5, and fluoranthene anion AGC = 4×10^5.

Former *N*-glycopeptides were separated using an identical chromatography setup to that described above, with detection using an LTQ-Orbitrap Velos (Thermo Scientific). An MS scan (400−2000 *m*/*z*; MS AGC = 1×10^6) was recorded in the Orbitrap set at a resolution of 30,000 at 400 *m*/*z* followed by data-dependent HCD MS/MS analysis of the ten most intense precursors. Parameters for acquiring HCD were identical to those described above except MS^n AGC = 1×10^5.

Analysis of Released *N*-Glycan MS Data

Monosaccharide compositions of the *N*-glycan structures were determined from precursor masses (200 ppm tolerance) of the acquired *N*-glycome data using the GlycMod tool (http://web.expasy.org/glycomod/) and verified with CID MS/MS where this was available (Supplementary Table 1). The CID MS/MS spectra were then manually annotated (Supplementary Figure 1), which together with the relative and absolute retention times of the *N*-glycans from the Hypercarb PGC column yielded further structural information such as glycan topology, sialic acid and fucose linkage type, and isobaric isomer formation.[44] MS/MS fragment ion masses and general knowledge of mammalian *N*-glycosylation were used to assign some of the structural aspects of the *N*-glycans; however, some structural ambiguity was still present for several *N*-glycans. The ambiguity is presented with brackets on *N*-glycan illustrations (Supplementary Table 1). On the basis of the precursor mass accuracy, PGC-LC retention time, and the quality of CID MS/MS spectra (i.e number of fragment ions assigned, fragment mass accuracy, and signal/noise levels), qualitative confidence levels for the observed *N*-glycans were given e.g., low, medium, and high. The relative abundance of each *N*-glycan isomer was manually determined from the relative extracted ion chromatogram (EIC) areas (EIC based on precursor ±0.5 *m*/*z*) for all observed charge states of the *N*-glycans out of the total EIC area sum of all *N*-glycans observed.

Analysis of Former *N*-Glycopeptide MS Data

Raw data were processed using Proteome Discoverer v1.3 (Thermo Scientific) into .mgf files and searched against UniProt *Rattus norvegicus* (March 2012: 41,696 entries) using the Mascot program (v2.4). Database searches were performed with the following fixed parameters: precursor mass tolerance of 20 ppm, product ion mass tolerance of 0.02 Da, carbamidomethylation of Cys, and 1 possible missed cleavage. Searches were also conducted with the following variable modifications: oxidation of Met and deamidation of Asn and Gln. All searches were filtered to <1% FDR using Percolator[47] and further filtered to contain Mascot ion scores >18. A nonredundant list of deamidated peptides along with their associated protein group accessions and protein descriptions was populated for each fraction. Peptides identified in each protein group accession were concatenated and a tryptic former glycopeptide-centric .fasta database created in Microsoft Excel for each fraction.

Analysis of Intact *N*-Glycopeptide MS Data

Raw data were processed using Proteome Discoverer v1.3 (Thermo Scientific) into separate .mgf files based on the fragmentation type for each fraction. For FT data peak-picking, signal-to-noise filtering was disabled. For ETD data, a nonfragment filter was applied to remove precursor and charge reduced precursor ions within 2 Da and to remove neutral losses less than 50 Da from charge reduced precursor ions within 2 Da. For HCD data, an in-house script was developed to separate the .mgf files into spectra containing an ion between 204.08−204.09. Glycopeptide spectra (HCD and ETD) from each fraction were searched against their corresponding concatenated peptide-centric .fasta database using Byonic software v1.09 (Protein Metrics).[48] Searches were performed with the following fixed modifications: precursor mass tolerance

dx.doi.org/10.1021/pr400783j | J. Proteome Res. 2013, 12, 5791−5800

of 20 ppm, product ion mass tolerance of 0.02 Da, carbamidomethylation of Cys, and fully specific cleavage (Byonic internally allows for mis-cleavages). Searches were also conducted with the following variable modifications: oxidation of Met and glycosylation of Asn with a potential 71 unique glycan compositions (Supplementary Table 1). Additional searches were performed against the *N*-glycan database available within Byonic with or without a precursor offset by one or two to account for incorrect monoisotopic peak selection. This is a particular issue for correct assignment of glycans containing 2 dHex (+292 Da) versus 1 NeuAc (+291 Da). This discrepancy was resolved by filtering spectra containing diagnostic NeuAc ions (274.09 and 292.10 *m*/*z*) and manual inspection of the correct monoisotopic peak (Supplementary Figure 2).

The HCD spectrum scan number, peak list, and peptide sequence of each of the peptide spectral matches (PSMs) identified by Byonic were extracted. The peak list and sequence was then used to automatically annotate spectra using the Expert System for Computer Assisted Annotation[49] using a 20 ppm product ion tolerance with fragment ion filtering disabled. Spectra were then queried to count the frequency of *b*- or *y*-type ion matches independent of ion intensity. This approach is particularly suited to the high-mass accuracy analysis of modified peptides containing multiple modifications or abundant oxonium/immonium ions that are not matched during database searching.[50] These abundant unmatched ions, as well as glycopeptide-related ions, attract a score penalty during database searching. Furthermore, lower abundant peptide backbone ions may not be matched. Annotation of the corresponding ETD spectra was performed in Byonic. Annotation of the corresponding CID spectra was performed manually if the attached *N*-glycan composition was identified with ≥2 structural glycan isomers from the released *N*-glycan analysis. For *N*-glycopeptides containing an attached *N*-glycan monosaccharide composition with ≥2 linkage isomers, the CID data were not annotated since these spectra are unable to distinguish between the *N*-glycan structures. Additionally, all assigned *N*-glycopeptide HCD spectra were checked to ensure the presence of further diagnostic HexNAc oxonium ions (138.055, 168.066, and 186.076 *m*/*z* ± 20 ppm).

RESULTS AND DISCUSSION

Overview of the Combination of Glycomics and Glycoproteomics

We have developed an analytical strategy capable of characterizing the heterogeneous membrane *N*-glycoproteome using the rat brain as a model (Figure 1). In brief, characterization of the membrane *N*-glycome (glycomics) facilitated subsequent site-specific glycan-peptide identification following enrichment, multidimensional liquid chromatography, analysis of formerly glycosylated and intact glycosylated peptides with high-resolution MS/MS employing complementary fragmentation techniques, and advanced data processing tools.

Orthogonal Fractionation of Glycopeptides Using RPLC

A tryptic digest of bovine fetuin was used to perform a preliminary investigation of the use of RPLC at pH 7.9 (10 mM ammonium bicarbonate) as a first dimension fractionation strategy for intact glycopeptides and its orthogonality with second dimension RPLC at pH 2.7 (0.1% formic acid). Five pmol fetuin tryptic digest was analyzed at the two different pH values using identical setups (the same C18AQ column and

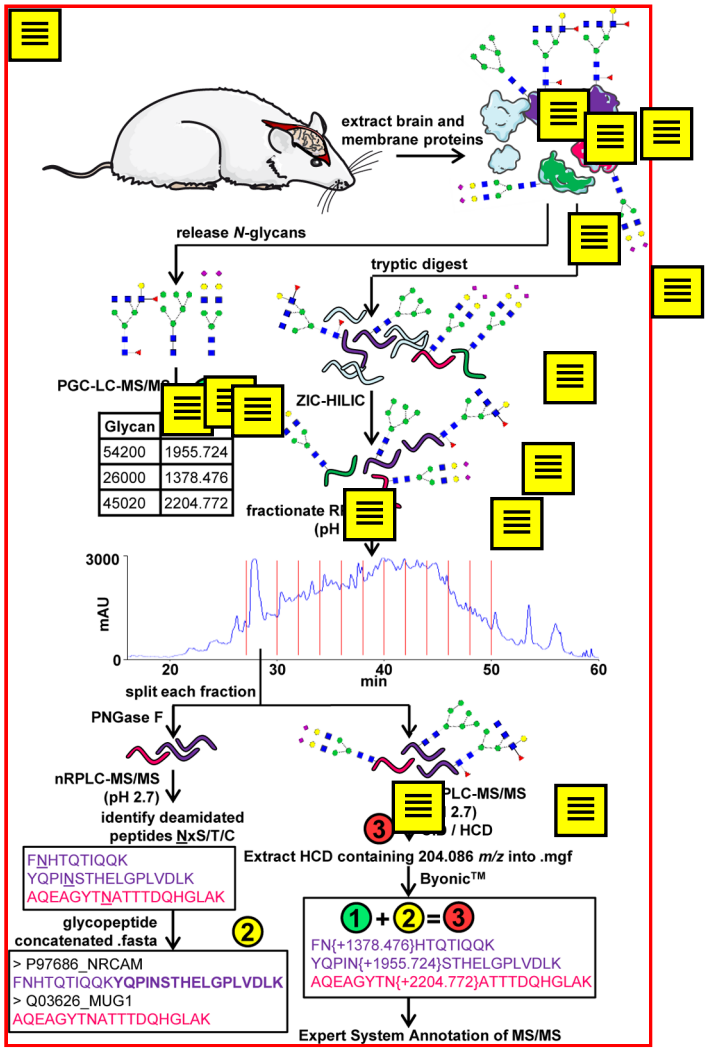

Figure 1. Site-specific *N*-glycosylation heterogeneity analysis of rat brain membrane-associated proteins by combining glycomics, glycoproteomics, and complementary mass spectrometry (MS) fragmentation techniques. Rat brains were extracted and membrane-associated proteins isolated. First, the *N*-glycome was defined using porous graphitized carbon high performance liquid chromatography–tandem mass spectrometry (PGC-LC–MS/MS). The monosaccharide compositions were used to create an *N*-glycan modification database. Next, an aliquot of membrane-associated proteins was digested with trypsin and glycopeptides enriched using zwitterionic-hydrophilic interaction liquid chromatography (Zic-HILIC). The enriched glycopeptides were fractionated using reversed-phase liquid chromatography (RPLC) (pH 7.9) and each fraction was split into two aliquots. The first aliquot was treated with PNGase F, which removes *N*-glycans with the diagnostic conversion of the *N*-linked asparagine (Asn) to an aspartic acid (Asp) by deamidation. Former glycopeptides were analyzed by nanoRPLC–MS/MS (pH 2.7) and identified by the observation of a deamidated Asn within the *N*-linked motif (NxS/T/C, x ≠ P). Glycopeptide sequences from each protein group were concatenated and a glycopeptide-centric database specific for each fraction created. Next, the second aliquot of each fraction was analyzed directly by nanoRPLC–MS/MS (pH 2.7) employing complementary fragmentation techniques. Spectra containing diagnostic HexNAc oxonium ions (*m*/*z* 204.086) were extracted and searched against the glycopeptide-centric databases using the *N*-glycan modification database to assign glycan compositions to the peptide sequence. Finally, MS/MS spectra were semiautomatically annotated using Expert System Annotation.

dx.doi.org/10.1021/pr400783j | *J. Proteome Res.* 2013, 12, 5791–5800

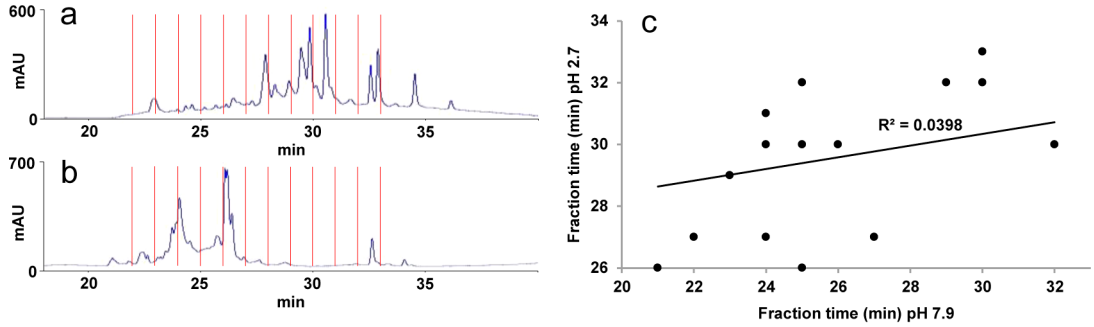

Figure 2. Orthogonal fractionations of a tryptic digest of bovine fetuin. (a) Reversed-phase liquid chromatography (RPLC) at pH 2.7 using 0.1% formic acid. (b) RPLC at pH 7.9 using 10 mM ammonium bicarbonate. (c) Comparison of the retention times of identified peptides between pH 2.7 and 7.9. Each point represents the fraction time (retention time) of a unique peptide sequence identified in both analyses.

gradient). Thirteen fractions were collected and were deglycosylated with PNGase F, which leaves a diagnostic mass tag through a deamidation reaction (Δm = 0.9840 Da, Asn to Asp conversion) upon *N*-glycan removal. Each fraction was analyzed by nanoRPLC–MS/MS (pH 2.7) employing CID, and the peptides present in each fraction were identified by Mascot with former *N*-glycosylated peptides identified by the observation of a deamidated Asn within the *N*-linked glycosylation motif (NxS/T/C, x ≠ P). Figure 2a,b shows the UV chromatograms of the analysis at the two different pH values highlighting large retention time differences. Figure 2c plots the retention times of the identified peptides in each fraction between the two different pH values (Supplementary Table 2). The nonlinear relationship highlights good orthogonality between the two different pH values as previously described.[51] Each unique former *N*-glycosylated peptide sequence was identified in a single fraction. This suggests that different glycoforms of the same peptide appear in a single fraction due to the peptide backbone moiety primarily defining the RP retention. Each fraction therefore contained the peptide sequence with all its associated glycoforms. We hypothesized that this strategy would greatly reduce the peptide complexity in each LC fraction. Identification of formerly glycosylated peptide sequences in each fraction would thus provide prior knowledge to minimize the search-space required for direct analysis of intact glycopeptides. Furthermore, the orthogonality of off-line first dimension RPLC fractionation of glycopeptides at pH 7.9 with online second dimension RPLC separation at pH 2.7 would maximize the number of MS/MS acquired.

N-Glycomic Analysis of the Rat Brain

Membrane-associated proteins were immobilized onto a PVDF membrane and glycans released with PNGase F. Released glycans were reduced and analyzed by PGC-LC–MS/MS resulting in the identification of 71 unique monosaccharide compositions, which were compiled into an *N*-glycan modification database (Supplementary Table 1 and Figure 1). Thirty-three monosaccharide compositions corresponded to a single *N*-glycan structure without any isomers, six displayed two or more topological (structural) glycan isomers (e.g., core fucosylation or outer-arm fucosylation), 13 displayed two or more linkage glycan isomers (e.g sialic acid linked α3 or α6 to galactose), and three displayed both linkage and topology isomers. Of the 71 unique monosaccharide compositions, 15 were observed at trace levels and were not characterized by MS/MS. In total, 89 unique *N*-glycan structures were identified (Table 1).

Analysis of *N*-Glycopeptides from Rat Brain

N-glycopeptides were enriched from a tryptic peptide mixture derived from the same preparation of rat brain membrane-associated proteins utilized for the *N*-glycome analysis. Glycopeptides were enriched using using Zic-HILIC[52,53] and separated into 13 fractions using off-line RPLC (pH 7.9). The resulting fractions were split into two equal aliquots and used for two separate analyses. The first analysis enabled identification of formerly glycosylated peptides after PNGase F catalyzed deglycosylation. The deglycosylated peptides were analyzed with acidic (pH 2.7) online nanoRPLC–MS/MS, and the former glycopeptides identified by the observation of a deamidated Asn within the conserved *N*-glycosylation motif (NxS/T/C, x ≠ P). In total, 1989 unique formerly glycosylated peptides were identified based on this analysis (Supplementary Table 3). From these data, a glycopeptide-centric concatenated database (.fasta) specific for each fraction was created and used to interpret the results of the subsequent analysis of intact *N*-glycopeptides. The second aliquot of each LC fraction containing intact *N*-glycopeptides was next directly analyzed by nanoRPLC-MS/MS employing collision induced dissociation (CID) and higher energy collision dissociation (HCD) fragmentation, which generate complementary structural information on intact glycopeptides.[54] HCD MS/MS spectra containing the diagnostic HexNAc oxonium ion (m/z 204.086 ± 20 ppm) were extracted from the entire pool of HCD MS/MS spectra. These intact glycopeptide spectra from each fraction were searched against the corresponding glycopeptide-centric concatenated .fasta files, combined with the defined *N*-glycan structure database obtained from the *N*-glycome analysis, using Byonic[48] software. A total of 2125 PSMs modified with an *N*-glycan were obtained by high mass accuracy precursor masses alone (± 20 ppm). Semiautomatic annotation of HCD MS/MS spectra was then performed using Expert System for Computer-Assisted Annotation[49] (Supplementary Figure 2). Annotated HCD MS/MS spectra were used to count the frequency of fragment ion matches within 20 ppm tolerance (*b*- or *y*-type) independent of ion intensity, which is efficient for assigning MS/MS spectra of modified peptides.[50] This simplified approach shows excellent sensitivity and specificity when combined with high mass accuracy.[55,56] To estimate the FDR for the glycopeptide identification, sequences of the PSMs were reversed (excluding the *C*-terminal Lys or Arg) and the frequency of ions matched to the reverse sequences determined. This resulted in the identification of 863 nonredundant *N*-glycopeptides (FDR = 1.8%; matched ions ≥ 4; Supplementary Figure 3) where both the peptide sequence

dx.doi.org/10.1021/pr400783j | *J. Proteome Res.* 2013, 12, 5791–5800

Table 1. Identified *N*-glycans from rat brain

Glycan #	Structure	monosaccharide composition (HexNAc, Hex, Fuc, NeuAc, NeuGc, Na)	Glycan #	Structure	monosaccharide composition (HexNAc, Hex, Fuc, NeuAc, NeuGc, Na)	Glycan #	Structure	monosaccharide composition (HexNAc, Hex, Fuc, NeuAc, NeuGc, Na)
1		231000	22b		541000	38a		541100
2		240000	22c		541000	38b		541100
3		250000	22d		541000	38c		541100
4		260000	23		631000	39	no MS/MS	561000
5		350000	24a		351100	40		642000
6		431000	24b	pooled with 24c	351100	41a	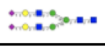	450200
7		530000	24c		351100	41b	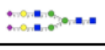	450200
7a		431000 + phos/sulf	25	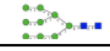	290000	42a	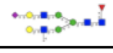	452100
8a		270000	26a	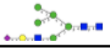	360100	42b	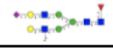	452100
8b	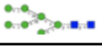	270000	26b	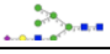	360100	43a		461100
9		351000	27	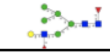	362000	43b	no MS/MS	461100
10	no MS/MS	360000	28a		441100	44	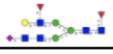	542100
11a		441000	28b		441100	45a	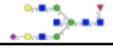	551100
11b	no MS/MS	441000	28c		441100	45b		551100
11c	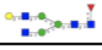	441000	28d		441100	46		553000
12		450000	29		452000	47a		641100
13		31000	30a		461000	47b	no MS/MS	641100
14		540000	30b		461000	48a		451200
15	no MS/MS	343000	31a		42000	48b		451200
16		280000	31b		42000	48c		1200
17		52000	32		551000	49a		552100
18a		361000	33a		1100	49b		552100
18b		531000 + phos/sulf	33b	pooled with 33c	51100	50		2200
19a		442000	33c		361100	51		564000
19b		2000	34		NA	52		552100
20a		451000	35a		51100	53		563100
20b	no MS/MS	451000	35b		51100	54		562200
20c		451000	36		453000	55a	poor MS/MS	663100
21		460000	37a	no MS/MS	462000	55b	no MS/MS	663100
22a		541000	37b		462000	56	poor MS/MS	662200

dx.doi.org/10.1021/pr400783j | *J. Proteome Res.* 2013, 12, 5791−5800

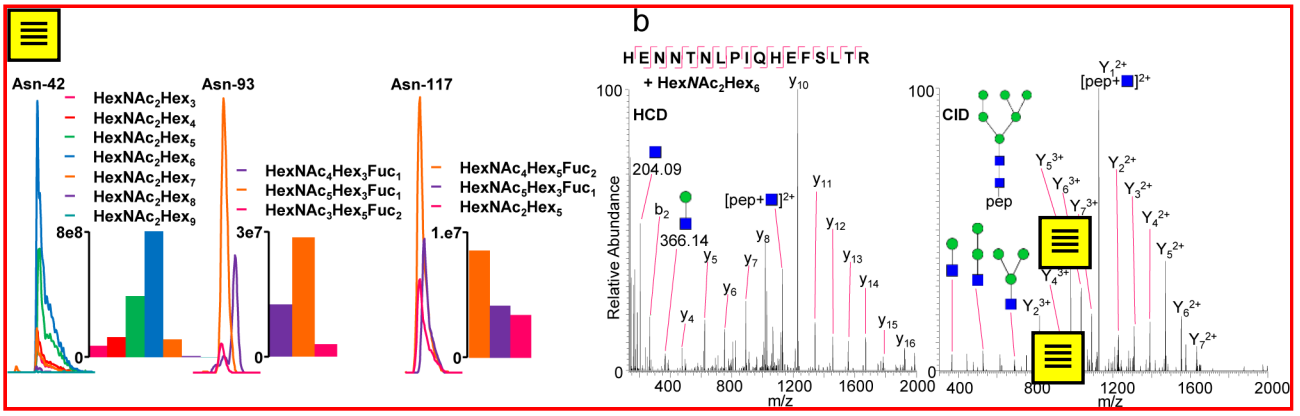

Figure 3. Site-specific *N*-glycosylation analysis of Thy-1 membrane glycoprotein (P01830) from rat brain. (a) Extracted ion chromatograms of *N*-glycopeptides identified from the three glycosylation sites at Asn-42, Asn-93, and Asn-117. Bar graphs show area under the curve for each glycopeptide identified. (b) HCD and CID MS/MS spectra of the major *N*-glycopeptide identified at Asn-42 containing Hex*N*Ac$_2$Hex$_6$. HCD predominantly shows peptide backbone fragmentation, while CID shows predominantly glycan fragmentation.

and attached glycan monosaccharide composition were determined (Supplementary Table 4 and Figure 2). Of these, 565 *N*-glycopeptides were modified with an *N*-glycan of monosaccharide composition corresponding to a single structure based on the *N*-glycome analysis. These identifications represent site-specific glycan structure assignments. Seventy-five *N*-glycopeptides were assigned a monosaccharide composition correlating to two or more *N*-glycan structural isomers. The corresponding CID MS/MS spectra of these were then interrogated for the presence of diagnostic ions allowing discrimination between *N*-glycan structural isomers of identical monosaccharide composition, e.g., discrimination between outer-arm fucosylation (diagnostic ion Hex*N*Ac$_1$Hex$_1$dHex$_1$; m/z = 512.2) and core fucosylation (identification of the peptide + Hex*N*Ac$_1$dHex$_1$ ion).[57] This resulted in the confident identification of 36 *N*-glycopeptide isoforms (i.e., same peptide with two or more structural glycan isomers attached) (Supplementary Table 4 and Figure 4). Then, 137 *N*-glycopeptides were modified with a glycan monosaccharide composition displaying two or more glycan linkage isomers that we were unable to resolve. The 863 positively identified glycopeptides covered 276 glycosylation sites on 161 protein groups.

Only 11 of the 161 identified proteins have been previously glyco-profiled in a site-specific manner, including only 2 from rat brain: Thy-1 membrane glycoprotein (Uniprot ID: P01830) and neurotrimin (Uniprot ID: Q62718). Rat Thy-1 has three *N*-glycosylation sites (Asn-42, Asn-93, and Asn-117).[58] Figure 3a shows EICs and the distribution of identified glycopeptides from rat Thy-1. Our results are consistent with previous studies where Asn-42 was reported to be occupied by high-mannose *N*-glycans (Hex*N*Ac$_2$Hex$_{5-6}$); Asn-93 by fucosylated complex-type *N*-glycans; and Asn-117 by fucosylated complex-type *N*-glycans and high-mannose.[59] HCD fragmentation yielded abundant peptide backbone fragment ions (b/y ions) with high mass accuracy, which enabled identification of peptide sequence and glycan monosaccharide composition, while CID fragmentation predominantly yielded glycosidic bond cleavages that substantiate the *N*-glycan structures (Figure 3b).

Site-specific glycosylation analysis of trans-membrane receptor proteins is particularly challenging due to their low abundance and often poor solubility. The analytical depth achieved with our strategy resulted in the characterization of 128 rat brain *N*-glycoproteins containing trans-membrane domains, which have not previously been glyco-profiled in a site-specific manner, including 25 CD antigens, 37 cell adhesion molecules, 27 transporters, and 13 peptidases (Supplementary Table 5).

Localization of glycosylation sites with amino acid residue resolution could not be determined analytically, and hence, we assumed the modification only occurred on Asn within the conserved *N*-glycosylation motif. As such, the analysis of a glycopeptide, which is comodified by both an *N*- and *O*-glycan may result in an incorrect assignment of the *N*-glycan monosaccharide composition at the *N*-linked site. To address this, ETD fragmentation of glycopeptides from six LC fractions was performed in conjunction with CID and HCD fragmentation. Unlike CID and HCD, ETD fragmentation yields cleavage of the peptide backbone with no glycan fragmentation, which is particularly suited to the localization of modified amino acids.[60] HCD resulted in the identification of 147 unique *N*-glycopeptides in this analysis (Supplementary Table 6 and Figure 5). ETD MS/MS spectra were then searched against the glycopeptide-centric concatenated database using Byonic with the *N*-glycan modification database defined from *N*-glycome analysis and an *O*-glycan modification database containing ~200 common *O*-glycan monosaccharide compositions (available within Byonic). Sixteen unique *N*-linked glycopeptides were identified with ≥4 c- or z-ions matched (± 20 ppm), and all of these were identified in the corresponding HCD MS/MS spectra (Supplementary Table 7 and Figure 6). No glycopeptides bearing both *N*- and *O*-glycans were identified.

■ CONCLUSIONS

This strategy combines the strength of in-depth *N*-glycan structure analysis with novel site-specific glycoproteomics workflows and data processing tools to address the previously unmet technical challenge of *N*-glycan-peptide heterogeneity determination from complex mammalian protein mixtures. The approach can be readily applied to other complex (glyco)-protein mixtures, and the high number of confident *N*-glycopeptide identifications from rat brain membrane glycoproteins represents the largest site-specific *N*-glycoproteome structural coverage achieved to date.

dx.doi.org/10.1021/pr400783j | *J. Proteome Res.* 2013, 12, 5791−5800

■ ASSOCIATED CONTENT

Supporting Information

PGC-LC−MS/MS and LC−MS/MS spectra and identified peptides. This material is available free of charge via the Internet at http://pubs.acs.org.

■ AUTHOR INFORMATION

Corresponding Author

*(B.L.P.) E-mail: b.parker@garvan.org.au. Phone: +6192958222. Fax: +6192958201.

Present Addresses

○Diabetes and Obesity Program and Biological Mass Spectrometry Unit, Garvan Institute of Medical Research, Darlinghurst, NSW 2010, Australia.

▽Centre for High-Throughput Biology, University of British Columbia, Vancouver, BC V6T 1Z4, Canada.

Notes

The authors declare no competing financial interest.

■ ACKNOWLEDGMENTS

This work was supported by the National Health and Medical Research Council (NHMRC) of Australia (to S.J.C., N.E.S., and M.E.G.), the Lundbeck Foundation, Denmark (to M.R.L.), the Cancer Institute, New South Wales (M.E.G.), and the Australian Research Council (ARC) (to M.T.-A.). We thank Marshall Bern, Matthew Campbell, Nadin Neuhauser, and Caupolican Solis for bioinformatics assistance and useful discussions.

■ REFERENCES

(1) Johansen, P. G.; Marshall, R. D.; Neuberger, A. Carbohydrates in protein. 3 The preparation and some of the properties of a glycopeptide from hen's-egg albumin. *Biochem. J.* **1961**, *78*, 518−27.

(2) Mizuochi, T.; Taniguchi, T.; Shimizu, A.; Kobata, A. Structural and numerical variations of the carbohydrate moiety of immunoglobulin G. *J. Immunol.* **1982**, *129* (5), 2016−20.

(3) Takahashi, N.; Ishii, I.; Ishihara, H.; Mori, M.; Tejima, S.; Jefferis, R.; Endo, S.; Arata, Y. Comparative structural study of the N-linked oligosaccharides of human normal and pathological immunoglobulin G. *Biochemistry* **1987**, *26* (4), 1137−44.

(4) Shields, R. L.; Lai, J.; Keck, R.; O'Connell, L. Y.; Hong, K.; Meng, Y. G.; Weikert, S. H.; Presta, L. G. Lack of fucose on human IgG1 N-linked oligosaccharide improves binding to human Fcgamma RIII and antibody-dependent cellular toxicity. *J. Biol. Chem.* **2002**, *277* (30), 26733−40.

(5) Shinkawa, T.; Nakamura, K.; Yamane, N.; Shoji-Hosaka, E.; Kanda, Y.; Sakurada, M.; Uchida, K.; Anazawa, H.; Satoh, M.; Yamasaki, M.; Hanai, N.; Shitara, K. The absence of fucose but not the presence of galactose or bisecting N-acetylglucosamine of human IgG1 complex-type oligosaccharides shows the critical role of enhancing antibody-dependent cellular cytotoxicity. *J. Biol. Chem.* **2003**, *278* (5), 3466−73.

(6) Lowe, J. B. Glycosylation, immunity, and autoimmunity. *Cell* **2001**, *104* (6), 809−12.

(7) Helenius, A.; Aebi, M. Intracellular functions of N-linked glycans. *Science* **2001**, *291* (5512), 2364−9.

(8) Rudd, P. M.; Elliott, T.; Cresswell, P.; Wilson, I. A.; Dwek, R. A. Glycosylation and the immune system. *Science* **2001**, *291* (5512), 2370−6.

(9) Wyss, D. F.; Choi, J. S.; Li, J.; Knoppers, M. H.; Willis, K. J.; Arulanandam, A. R.; Smolyar, A.; Reinherz, E. L.; Wagner, G. Conformation and function of the N-linked glycan in the adhesion domain of human CD2. *Science* **1995**, *269* (5228), 1273−8.

(10) Wormald, M. R.; Dwek, R. A. Glycoproteins: glycan presentation and protein-fold stability. *Structure* **1999**, *7* (7), R155−60.

(11) Jakob, C. A.; Burda, P.; Roth, J.; Aebi, M. Degradation of misfolded endoplasmic reticulum glycoproteins in Saccharomyces cerevisiae is determined by a specific oligosaccharide structure. *J. Cell Biol.* **1998**, *142* (5), 1223−33.

(12) Chen, J.; Moloney, D. J.; Stanley, P. Fringe modulation of Jagged1-induced Notch signaling requires the action of beta 4galactosyltransferase-1. *Proc. Natl. Acad. Sci. U.S.A.* **2001**, *98* (24), 13716−21.

(13) Moody, A. M.; Chui, D.; Reche, P. A.; Priatel, J. J.; Marth, J. D.; Reinherz, E. L. Developmentally regulated glycosylation of the CD8alphabeta coreceptor stalk modulates ligand binding. *Cell* **2001**, *107* (4), 501−12.

(14) Kaji, H.; Saito, H.; Yamauchi, Y.; Shinkawa, T.; Taoka, M.; Hirabayashi, J.; Kasai, K.; Takahashi, N.; Isobe, T. Lectin affinity capture, isotope-coded tagging and mass spectrometry to identify N-linked glycoproteins. *Nat. Biotechnol.* **2003**, *21* (6), 667−72.

(15) Zhang, H.; Li, X. J.; Martin, D. B.; Aebersold, R. Identification and quantification of N-linked glycoproteins using hydrazide chemistry, stable isotope labeling and mass spectrometry. *Nat. Biotechnol.* **2003**, *21* (6), 660−6.

(16) Zielinska, D. F.; Gnad, F.; Wisniewski, J. R.; Mann, M. Precision mapping of an in vivo N-glycoproteome reveals rigid topological and sequence constraints. *Cell* **2010**, *141* (5), 897−907.

(17) Wada, Y.; Azadi, P.; Costello, C. E.; Dell, A.; Dwek, R. A.; Geyer, H.; Geyer, R.; Kakehi, K.; Karlsson, N. G.; Kato, K.; Kawasaki, N.; Khoo, K. H.; Kim, S.; Kondo, A.; Lattova, E.; Mechref, Y.; Miyoshi, E.; Nakamura, K.; Narimatsu, H.; Novotny, M. V.; Packer, N. H.; Perreault, H.; Peter-Katalinic, J.; Pohlentz, G.; Reinhold, V. N.; Rudd, P. M.; Suzuki, A.; Taniguchi, N. Comparison of the methods for profiling glycoprotein glycans–HUPO Human Disease Glycomics/Proteome Initiative multi-institutional study. *Glycobiology* **2007**, *17* (4), 411−22.

(18) Royle, L.; Campbell, M. P.; Radcliffe, C. M.; White, D. M.; Harvey, D. J.; Abrahams, J. L.; Kim, Y. G.; Henry, G. W.; Shadick, N. A.; Weinblatt, M. E.; Lee, D. M.; Rudd, P. M.; Dwek, R. A. HPLC-based analysis of serum N-glycans on a 96-well plate platform with dedicated database software. *Anal. Biochem.* **2008**, *376* (1), 1−12.

(19) Isailovic, D.; Kurulugama, R. T.; Plasencia, M. D.; Stokes, S. T.; Kyselova, Z.; Goldman, R.; Mechref, Y.; Novotny, M. V.; Clemmer, D. E. Profiling of human serum glycans associated with liver cancer and cirrhosis by IMS-MS. *J. Proteome Res.* **2008**, *7* (3), 1109−17.

(20) Morelle, W.; Stechly, L.; Andre, S.; Van Seuningen, I.; Porchet, N.; Gabius, H. J.; Michalski, J. C.; Huet, G. Glycosylation pattern of brush border-associated glycoproteins in enterocyte-like cells: involvement of complex-type N-glycans in apical trafficking. *Biol. Chem.* **2009**, *390* (7), 529−44.

(21) Pabst, M.; Wu, S. Q.; Grass, J.; Kolb, A.; Chiari, C.; Viernstein, H.; Unger, F. M.; Altmann, F.; Toegel, S. IL-1beta and TNF-alpha alter the glycophenotype of primary human chondrocytes in vitro. *Carbohydr. Res.* **2010**, *345* (10), 1389−93.

(22) Nakano, M.; Saldanha, R.; Gobel, A.; Kavallaris, M.; Packer, N. H. Identification of glycan structure alterations on cell membrane proteins in desoxyepothilone B resistant leukemia cells. *Mol. Cell. Proteomics* **2011**, *10* (11), M111 009001.

(23) Thomsson, K. A.; Backstrom, M.; Holmen Larsson, J. M.; Hansson, G. C.; Karlsson, H. Enhanced detection of sialylated and sulfated glycans with negative ion mode nanoliquid chromatography/mass spectrometry at high pH. *Anal. Chem.* **2010**, *82* (4), 1470−7.

(24) Staples, G. O.; Shi, X.; Zaia, J. Glycomics analysis of mammalian heparan sulfates modified by the human extracellular sulfatase HSulf2. *PLoS One* **2011**, *6* (2), e16689.

(25) Zauner, G.; Koeleman, C. A.; Deelder, A. M.; Wuhrer, M. Mass spectrometric O-glycan analysis after combined O-glycan release by beta-elimination and 1-phenyl-3-methyl-5-pyrazolone labeling. *Biochim. Biophys. Acta* **2012**, *1820* (9), 1420−8.

(26) Walther, T.; Karamanska, R.; Chan, R. W.; Chan, M. C.; Jia, N.; Air, G.; Hopton, C.; Wong, M. P.; Dell, A.; Malik Peiris, J. S.; Haslam, S. M.; Nicholls, J. M. Glycomic analysis of human respiratory tract tissues and correlation with influenza virus infection. *PLoS Pathog.* **2013**, *9* (3), e1003223.
(27) An, H. J.; Peavy, T. R.; Hedrick, J. L.; Lebrilla, C. B. Determination of N-glycosylation sites and site heterogeneity in glycoproteins. *Anal. Chem.* **2003**, *75* (20), 5628−37.
(28) Faid, V.; Evjen, G.; Tollersrud, O. K.; Michalski, J. C.; Morelle, W. Site-specific glycosylation analysis of the bovine lysosomal alpha-mannosidase. *Glycobiology* **2006**, *16* (5), 440−61.
(29) Kolarich, D.; Weber, A.; Turecek, P. L.; Schwarz, H. P.; Altmann, F. Comprehensive glyco-proteomic analysis of human alpha1-antitrypsin and its charge isoforms. *Proteomics* **2006**, *6* (11), 3369−80.
(30) Kuzmanov, U.; Jiang, N.; Smith, C. R.; Soosaipillai, A.; Diamandis, E. P. Differential N-glycosylation of kallikrein 6 derived from ovarian cancer cells or the central nervous system. *Mol. Cell. Proteomics* **2009**, *8* (4), 791−8.
(31) West, M. B.; Segu, Z. M.; Feasley, C. L.; Kang, P.; Klouckova, I.; Li, C.; Novotny, M. V.; West, C. M.; Mechref, Y.; Hanigan, M. H. Analysis of site-specific glycosylation of renal and hepatic gamma-glutamyl transpeptidase from normal human tissue. *J. Biol. Chem.* **2010**, *285* (38), 29511−24.
(32) Yu, T.; Guo, C.; Wang, J.; Hao, P.; Sui, S.; Chen, X.; Zhang, R.; Wang, P.; Yu, G.; Zhang, L.; Dai, Y.; Li, N. Comprehensive characterization of the site-specific N-glycosylation of wild-type and recombinant human lactoferrin expressed in the milk of transgenic cloned cattle. *Glycobiology* **2011**, *21* (2), 206−24.
(33) Korekane, H.; Korekane, A.; Yamaguchi, Y.; Kato, M.; Miyamoto, Y.; Matsumoto, A.; Hasegawa, T.; Suzuki, K.; Taniguchi, N.; Ookawara, T. N-Glycosylation profiling of recombinant mouse extracellular superoxide dismutase produced in Chinese hamster ovary cells. *Glycoconjugate J.* **2011**, *28* (3−4), 183−96.
(34) Sumer-Bayraktar, Z.; Kolarich, D.; Campbell, M. P.; Ali, S.; Packer, N. H.; Thaysen-Andersen, M. N-glycans modulate the function of human corticosteroid-binding globulin. *Mol. Cell. Proteomics* **2011**, *10* (8), M111 009100.
(35) Liu, Y. C.; Yen, H. Y.; Chen, C. Y.; Chen, C. H.; Cheng, P. F.; Juan, Y. H.; Khoo, K. H.; Yu, C. J.; Yang, P. C.; Hsu, T. L.; Wong, C. H. Sialylation and fucosylation of epidermal growth factor receptor suppress its dimerization and activation in lung cancer cells. *Proc. Natl. Acad. Sci. U.S.A.* **2011**, *108* (28), 11332−7.
(36) Thaysen-Andersen, M.; Packer, N. H. Site-specific glycoproteomics confirms that protein structure dictates formation of N-glycan type, core fucosylation and branching. *Glycobiology* **2012**, *22* (11), 1440−52.
(37) Uematsu, R.; Furukawa, J.; Nakagawa, H.; Shinohara, Y.; Deguchi, K.; Monde, K.; Nishimura, S. High throughput quantitative glycomics and glycoform-focused proteomics of murine dermis and epidermis. *Mol Cell Proteomics* **2005**, *4* (12), 1977−89.
(38) Nilsson, J.; Ruetschi, U.; Halim, A.; Hesse, C.; Carlsohn, E.; Brinkmalm, G.; Larson, G. Enrichment of glycopeptides for glycan structure and attachment site identification. *Nat. Methods* **2009**, *6* (11), 809−11.
(39) Steentoft, C.; Vakhrushev, S. Y.; Vester-Christensen, M. B.; Schjoldager, K. T.; Kong, Y.; Bennett, E. P.; Mandel, U.; Wandall, H.; Levery, S. B.; Clausen, H. Mining the O-glycoproteome using zinc-finger nuclease-glycoengineered SimpleCell lines. *Nat. Methods* **2011**, *8* (11), 977−82.
(40) Halim, A.; Nilsson, J.; Ruetschi, U.; Hesse, C.; Larson, G. Human urinary glycoproteomics; attachment site specific analysis of N- and O-linked glycosylations by CID and ECD. *Mol. Cell. Proteomics* **2012**, *11* (4), 013649.
(41) Darula, Z.; Sherman, J.; Medzihradszky, K. F. How to dig deeper? Improved enrichment methods for mucin core-1 type glycopeptides. *Mol. Cell. Proteomics* **2012**, *11* (7), O111 016774.
(42) Yin, X.; Bern, M.; Xing, Q.; Ho, J.; Viner, R.; Mayr, M. Glycoproteomic analysis of the secretome of human endothelial cells. *Mol. Cell. Proteomics* **2013**, *12* (4), 956−78.
(43) Trinidad, J. C.; Schoepfer, R.; Burlingame, A. L.; Medzihradszky, K. F. N- and O-glycosylation in the murine synaptosome. *Mol. Cell. Proteomics* **2013**, DOI: 10.1074/mcp.M113.030007.
(44) Jensen, P. H.; Karlsson, N. G.; Kolarich, D.; Packer, N. H. Structural analysis of N- and O-glycans released from glycoproteins. *Nat. Protoc.* **2012**, *7* (7), 1299−310.
(45) Hao, P.; Ren, Y.; Alpert, A. J.; Sze, S. K. Detection, evaluation and minimization of nonenzymatic deamidation in proteomic sample preparation. *Mol. Cell. Proteomics* **2011**, *10* (10), O111 009381.
(46) Palmisano, G.; Melo-Braga, M. N.; Engholm-Keller, K.; Parker, B. L.; Larsen, M. R. Chemical deamidation: a common pitfall in large-scale N-linked glycoproteomic mass spectrometry-based analyses. *J. Proteome Res.* **2012**, *11* (3), 1949−57.
(47) Kall, L.; Canterbury, J. D.; Weston, J.; Noble, W. S.; MacCoss, M. J. Semi-supervised learning for peptide identification from shotgun proteomics datasets. *Nat. Methods* **2007**, *4* (11), 923−5.
(48) Bern, M.; Kil, Y. J.; Becker, C. Byonic: advanced Peptide and protein identification software. In *Current Protocols in Bioinformatics*; Wiley: New York, 2012; Chapter 13, Unit 13.20.
(49) Neuhauser, N.; Michalski, A.; Cox, J.; Mann, M. Expert System for Computer Assisted Annotation of MS/MS Spectra. *Mol Cell Proteomics* **2012**, *11*, 1500−1509.
(50) Savitski, M. M.; Mathieson, T.; Becher, I.; Bantscheff, M. H-score, a mass accuracy driven rescoring approach for improved peptide identification in modification rich samples. *J. Proteome Res.* **2010**, *9* (11), 5511−6.
(51) Gilar, M.; Olivova, P.; Daly, A. E.; Gebler, J. C. Orthogonality of separation in two-dimensional liquid chromatography. *Anal. Chem.* **2005**, *77* (19), 6426−34.
(52) Hagglund, P.; Bunkenborg, J.; Elortza, F.; Jensen, O. N.; Roepstorff, P. A new strategy for identification of N-glycosylated proteins and unambiguous assignment of their glycosylation sites using HILIC enrichment and partial deglycosylation. *J. Proteome Res.* **2004**, *3* (3), 556−66.
(53) Mysling, S.; Palmisano, G.; Hojrup, P.; Thaysen-Andersen, M. Utilizing ion-pairing hydrophilic interaction chromatography solid phase extraction for efficient glycopeptide enrichment in glycoproteomics. *Anal. Chem.* **2010**, *82* (13), 5598−609.
(54) Scott, N. E.; Parker, B. L.; Connolly, A. M.; Paulech, J.; Edwards, A. V.; Crossett, B.; Falconer, L.; Kolarich, D.; Djordjevic, S. P.; Hojrup, P.; Packer, N. H.; Larsen, M. R.; Cordwell, S. J. Simultaneous glycan-peptide characterization using hydrophilic interaction chromatography and parallel fragmentation by CID, higher energy collisional dissociation, and electron transfer dissociation MS applied to the N-linked glycoproteome of Campylobacter jejuni. *Mol. Cell. Proteomics* **2011**, *10* (2), M000031−MCP201.
(55) Wenger, C. D.; Coon, J. J. A proteomics search algorithm specifically designed for high-resolution tandem mass spectra. *J. Proteome Res.* **2013**, *12* (3), 1377−86.
(56) Peterson, A. C.; Russell, J. D.; Bailey, D. J.; Westphall, M. S.; Coon, J. J. Parallel reaction monitoring for high resolution and high mass accuracy quantitative, targeted proteomics. *Mol. Cell. Proteomics* **2012**, *11* (11), 1475−88.
(57) Wuhrer, M.; Koeleman, C. A.; Hokke, C. H.; Deelder, A. M. Mass spectrometry of proton adducts of fucosylated N-glycans: fucose transfer between antennae gives rise to misleading fragments. *Rapid Commun. Mass Spectrom.* **2006**, *20* (11), 1747−54.
(58) Parekh, R. B.; Tse, A. G.; Dwek, R. A.; Williams, A. F.; Rademacher, T. W. Tissue-specific N-glycosylation, site-specific oligosaccharide patterns and lentil lectin recognition of rat Thy-1. *EMBO J.* **1987**, *6* (5), 1233−44.
(59) Williams, A. F.; Parekh, R. B.; Wing, D. R.; Willis, A. C.; Barclay, A. N.; Dalchau, R.; Fabre, J. W.; Dwek, R. A.; Rademacher, T. W. Comparative analysis of the N-glycans of rat, mouse and human Thy-1. Site-specific oligosaccharide patterns of neural Thy-1, a member of the immunoglobulin superfamily. *Glycobiology* **1993**, *3* (4), 339−48.

(60) Hogan, J. M.; Pitteri, S. J.; Chrisman, P. A.; McLuckey, S. A. Complementary structural information from a tryptic N-linked glycopeptide via electron transfer ion/ion reactions and collision-induced dissociation. *J. Proteome Res.* **2005**, *4* (2), 628−32.